

Localization-enhanced dissipation in a generalized Aubry-André-Harper model coupled with Ohmic baths

H. T. Cui ^{1,*}, M. Qin ^{1,†}, L. Tang ¹, H. Z. Shen ², and X. X. Yi ^{2‡}

¹ *School of Physics and Optoelectronic Engineering, Ludong University, Yantai 264025, China and*

² *Center for Quantum Sciences, Northeast Normal University, Changchun 130024, China*

(Dated: July 28, 2022)

In this work, the exact dynamics of excitation in the generalized Aubry-André-Harper model coupled with an Ohmic-type environment is discussed by evaluating the survival probability and inverse participation ratio of the state of system. In contrast to the common belief that localization will preserve the information of the initial state in the system against dissipation into the environment, our study found that strong localization can enhance the dissipation of quantum information instead. By a thorough examination of the dynamics, we show that the coherent transition between the energy state of system is crucial for understanding this unusual behavior. Under this circumstance, the coupling induced energy exchange between the system and its environment can induce the periodic population of excitation on the states of system. As a result, the stable or localization-enhanced decaying of excitation can be observed, dependent on the energy difference between the states of system. This point is verified in further by checking the varying of dynamics of excitation in the system when the coupling between the system and environment is more strong.

I. INTRODUCTION

The closed quantum system can display resistance to the thermalization under its own intrinsic dynamics when it is localized, e.g., induced by static disorder[1], a linear potential with a spatial gradient [2], or the presence of a special subspace of the Hilbert space[3, 4]. Experimental evidence for the violation of ergodicity was presented, e.g., in ultracold atomic fermions [5] and superconducting systems [6]. In practice, no realistic systems can be immune to environmental coupling. Recent studies have found that even when the system is eventually driven to the thermal equilibrium, the localization decays slowly [7]. This strained localization decay induces a large time window during which the nonergodic character of the system becomes apparent [8].

While localization will be detrimental to the transportation of quantum particles in systems, it was recently discovered that increasing disorder within a system can enhance particle transport [9]. Furthermore, combined with environment-induced dephasing, the localized system can display robust quantum transport [10]. These findings imply that the interplay of localization and environment-induced decoherence can give rise to intriguing and complex dynamics in quantum systems. It motivates us to reconsider the robustness of localization, based on a fundamental point that the system is dissipative because of coupling to the environment. For this purpose, we studied the exact evolution of single excitation in a one-dimensional lattice system coupled to a bosonic environment. Different from Markovian treatments in previous works [7], the exact dynamics of exci-

tation can display strong dissipation or stable oscillation, depending on the localization of initial state. Moreover, we found that strong localization may enhance the decaying of excitation, rather than preserve excitation in the system. We argue that this counter intuitive feature is a consequence of the energy exchange between the system and environment, which induces the coherent transition in the energy levels of system.

The work is divided into five sections. Following the preceding introduction, section II introduces the model, and the dynamic equation for excitation is derived. In section III, we discuss the time evolution of excitation for different cases by calculating the survival probability of the information of initial state and the inverse participation ratio, both of which characterize the localization of system. Subsequently, a physical explanation is provided in section IV. It is shown that the energy exchange between the system and environment is responsible for the unusual observation. Finally, conclusion is presented in section V.

II. THE MODEL AND DYNAMIC EQUATION

In this work, we focus on the open dynamics of single excitation in a generalized Aubry-André-Harper (GAAH) model described by the Hamiltonian below [11]

$$H_S = \lambda \sum_{n=1}^N \left(c_n^\dagger c_{n+1} + c_{n+1}^\dagger c_n \right) + \Delta \frac{\cos(2\pi\beta n + \phi)}{1 - a \cos(2\pi\beta n + \phi)} c_n^\dagger c_n, \quad (1)$$

where N denotes the number of lattice sites and c_n (c_n^\dagger) is the annihilation (creation) operator of excitation at the n -th lattice site. For a quasi-periodic modulation, we adopt $\beta = (\sqrt{5} - 1)/2$ with respect to the recent exper-

*Electronic address: cuiht01335@aliyun.com

†Electronic address: qinming@ldu.edu.cn

‡Electronic address: yixx@nenu.edu.cn

imental verification of delocalization- localization transition [5]. The onsite potential is a smooth function of parameter a in open interval $a \in (-1, 1)$. When $a = 0$, Eq. (1) reduces to the standard AAH model [12], in which a delocalization- localization phase transition can occur when $\Delta = 2\lambda$. Whereas for $a \neq 0$, GHHA exhibits an exact mobility edge (ME) following the expression [11]

$$aE_c = \text{sign}(\lambda)(2|\lambda| - |\Delta|). \quad (2)$$

In the above, E_c is a special eigenenergy of H_S , that separates the extended eigenstates from localized counterparts. The coexistence of localized and delocalized states is a typical feature of GAAH model, and leads to the complex excitation dynamics in the system. To avoid the boundary effect, the periodic boundary condition, i.e., $c_n = c_{n+N}$, is adopted. Since the current work focuses on the robustness of localization in the system, $\phi = \pi$ is adopt without a loss of generality. For simplicity, $\hbar = \lambda \equiv 1$ is assumed in the following discussion. Recently, the localization properties of GAAH model has been experimentally investigated in optical lattices [13].

To establish the open dynamics of localization in the GAAH model, bosonic reservoir with different modes characterized by frequency ω_k are introduced as the environment. Its Hamiltonian can be written as follows:

$$H_B = \sum_k \omega_k b_k^\dagger b_k, \quad (3)$$

where b_k (b_k^\dagger) is the annihilation (creation) operator of reservoir k . The system is coupled to the environment via particle-particle exchanging,

$$H_{int} = \sum_{k,n} \left(g_k b_k c_n^\dagger + g_k^* b_k^\dagger c_n \right) \quad (4)$$

where g_k is the coupling amplitude between the system and reservoir mode k . The complexity of dynamics is determined by the spectral density

$$J(\omega) = \sum_k |g_k|^2 \delta(\omega - \omega_k), \quad (5)$$

which characterizes the energy structure of the system plus the system-environment interaction. In this work, Ohmic-type spectral density is adopt as follows:

$$J(\omega) = \eta \omega \left(\frac{\omega}{\omega_c} \right)^{s-1} e^{-\omega/\omega_c}. \quad (6)$$

The quantity η is simply the classical friction coefficient, and thus forms a dimensionless measure of the coupling strength between the system and its environment [14]. Actually, Eq. (6) characterizes the damping movement of electrons in a potential, and can simulate a large class of environments. The environment can be classified as sub-Ohmic ($s < 1$), Ohmic ($s = 1$) or super-Ohmic ($s > 1$) [14]. Without loss of generality, we focus on the Ohmic case ($s = 1$) since it characterizes the typical dynamics

of dissipation in the system [14]. Here, ω_c is the cutoff frequency of the environment spectrum, beyond which the spectral density starts to fall off; hence, it determines the regime of reservoir frequency, which is dominant for dissipation. In general, the value of ω_c depends on the specific environment. In this work, $\omega_c = 10$ is set in order to guarantee that the highest energy level in H_S is embedded into the continuum of the environment.

With respect of the absence of particle interaction in Eq.(1), it is convenient to focus our attention on the dynamics of single excitation. Under this prerequisite, the environment is set to be at zero temperature such that it can be at vacuum state. With respect of the environment at finite-temperature, the recent studies have shown that the localization may be destroyed by heating dynamics. As a result, the system relaxes eventually into a infinite-temperature state [7]. However, the relaxation is logarithmically slow in time because of the localization in system [7]. This means that there is a time window where the nonergodic feature of localization can be observed in experiments [8]. So it is expected that the dynamics of localization can display some unusual feature at zero temperature because of the strong coupling between system and environment. Furthermore, the dynamics of localization can be treated exactly in this case. And thus one can get a comprehensive picture how the localization in the system is varied by coupling to environment. For this purpose, the dynamical equations of excitation must be derived first. Formally, at any time t , the state of the system plus environment can be written as

$$|\psi(t)\rangle = \left(\sum_{n=1}^N \alpha_n(t) |1\rangle_n |0\rangle^{\otimes(N-1)} \right) \otimes |0\rangle^{\otimes M} + |0\rangle^{\otimes N} \otimes \left(\sum_{k=1}^M \beta_k(t) |1\rangle_k |0\rangle^{\otimes(M-1)} \right), \quad (7)$$

where $|1\rangle_n = c_n^\dagger |0\rangle_n$ denotes the occupation of the n -th lattice site, $|0\rangle_k$ is the vacuum state of b_k and $|1\rangle_k = b_k^\dagger |0\rangle_k$, and M denotes the number of mode in the environment. Substituting Eq. (7) into Schrödinger equation and solving first for $\beta_k(t)$, one can get a integrodifferential equation for $\alpha_n(t)$,

$$\begin{aligned} \mathbf{i} \frac{\partial}{\partial t} \alpha_n(t) &= [\alpha_{n+1}(t) + \alpha_{n-1}(t)] + \Delta \cos(2\pi\beta n + \phi) \alpha_n(t) \\ &\quad - \mathbf{i} \sum_{n=1}^N \int_0^t d\tau \alpha_n(\tau) f(t - \tau), \end{aligned} \quad (8)$$

where \mathbf{i} is the square root of -1 , and the memory kernel $f(t - \tau)$ is defined as

$$f(t - \tau) = \int_0^\infty d\omega J(\omega) e^{-\mathbf{i}\omega(t-\tau)}. \quad (9)$$

It is evident that the population amplitude of $\alpha_n(t)$ is significantly correlated to its past values. For spectral

density shown in Eq. (6), $f(t-\tau) = \frac{\eta}{\omega_c^{s-1}} \frac{\Gamma(s+1)}{[i(t-\tau)+1/\omega_c]^{s+1}}$. It is noted that the Markovian limit could be obtained by replacing $\alpha_n(\tau)$ in Eq. (8) with its current value $\alpha_n(t)$. As a result, the last term on the right hand of Eq. (7) contributes a positive term to Eq. (8), which depicts the decaying of $\alpha_n(t)$ [15]. So, it is expected that the non-Markovian feature would inspire the distinct dynamics of excitation.

III. DYNAMICAL EVOLUTION OF EXCITATION IN THE SYSTEM

Taking the existence of ME into account, we focus on the evolution of excitation initially in the highest excited eigenstate (ES) of H_S [13]. Thus, as for Eq. (2), the higher eigenenergy refers to the stronger localization in the ES [11]. Moreover, since ES is embedded in the continuum of the environment, the occurrence of a bound state is excluded from the current discussion [17]. We introduce the survival probability (SP), defined as $SP = |\langle \psi(t) | ES \rangle|^2$, to characterize the dissipation of quantum information. In addition, the inverse participation ratio (IPR), defined as $IPR = \sum_{n=1}^N |\alpha_n(t)|^4$, is also calculated to establish localization variation in the system. Both SP and IPR have been extensively used to explore the dynamics of localization in disordered many-body systems [16].

The following discussion focuses on two cases, i.e., $a = 0$ and $a = 0.5$. For the former case, ME is absent. However, a delocalization-localization transition can occur in the system when $\Delta = 2$, which separates the delocalized ($\Delta < 2$) from the localized ($\Delta > 2$) phase. This transition is absent in the latter; instead, the eigenstates are classified as localized ($E > E_c$) or extended ($E < E_c$) since the occurrence of ME.

Finally, the difficulty of finding the analytical solution to Eq. (8) is noted. Thus, we have to rely on numeric method. Our method is to transform the integral in Eq. (8) into a summation with properly chosen step length. By solving Eq. (8) iteratively, $\alpha_n(t)$ could be determined for any times t . However, the computational cost grows exponentially as the number of steps and lattices number N . To disclose the long-time behavior of SP and IPR, N is restricted to 21 so that $t = 1, 200$ could be achieved in a moderate computational cost.

A. $a = 0$

In Fig. 1, the time evolution of SP and IPR is plotted for different values of Δ . As shown in Fig.1(a1) and (a2), both SR and IPR indicate a rapid decaying when the system is in a delocalized phase ($\Delta < 2$). With an increase of Δ , the decay of IPR becomes very slow, as shown in Fig.1(a2). Meanwhile, a stable oscillation is developed for SP, as indicated for $\Delta = 2.5$ in Fig. 1(a1) and $\Delta = 3$ and 4 in Fig. 1(b1). Whereas ES is localized

in these cases, it manifests the robustness of localization against dissipation. This finding is different from the observation in Refs.[7], where the localized system eventually reflect a thermal equilibrium because of coupling to the environment. It can be attributed to the effect of memory kernel $f(t-\tau)$, which makes the past and current state of system interfered. The stability of SP or IPR can also be manifested by finding the variance of the position of excitation within the atomic site, $\langle \delta^2 n \rangle$. As show in Fig.A2(b) in Appendix, $\langle \delta^2 n \rangle$ displays a regular oscillation for $\Delta = 2.5$. In contrast, it becomes irregular for $\Delta = 1$ shown in Fig.A2(a).

With a further increase in Δ , we find that both SP and IPR reflect significant decaying, as shown for $\Delta = 6$ and 10 in Fig.1(b1) and (b2). This unusual feature indicates that the strong localization may have enhanced the loss of quantum information, rather than preserving it against decoherence. However, we also note that, in contrast to the super-exponential decaying of the extended state, the strongly localized state decays exponentially instead. Experimentally, this implies that it is still possible to differentiate the extended from the localized phase by checking the process of decoherence. In addition, it is noted that $\langle \delta^2 n \rangle$ can tend to be steady shown in Fig.A2(c). This observation can be considered as a result of the strong localization in the system.

B. $a = 0.5$

To gain a further understanding of the localization-enhanced dissipation, this section focuses on the case of $a \neq 0$. A distinct feature in this situation is the occurrence of ME [11]. Consequently, the energy ES of H_S may behave in a localized or extended manner, which will be decided by the relationship of eigenvalue E and E_c in Eq. (2). As a result, the system cannot simply be classified as either localized or extended. It is noted that, depending on the sign of a , the maximally localized state can be exchanged between the ground state and the highest excited state of H_S [11]. Since this work focuses on the interplay of localization and dissipation, $a = 0.5$ is selected as an exemplification. Accordingly, ES has the largest localization. For $a < 0$, the ground state is maximally localized instead. For $\omega_k > 0$, the coupling to the environment renormalizes the ground state as a dissipationless bound state [17]. This unique situation is excluded from our discussion.

In Fig. 2, the evolution of SR and IPR are presented for different values of Δ . Two selected cases, i.e., $\Delta = 0.5$ and 0.76 are first studied, for which ES is extended or has the eigenvalue very closed to E_c . Both SP and IPR display rapidly decaying at an earlier time before very slowly descending, as shown in Fig. 2 (a1) and (a2). With the increase of Δ , ES behaves in a more localized manner. As is anticipated, it is noted that both SP and IPR decay slowly when $\Delta = 1.5, 2$ and 3. In contrast, a steep descent is observed when $\Delta = 3, 6$ and 10, as

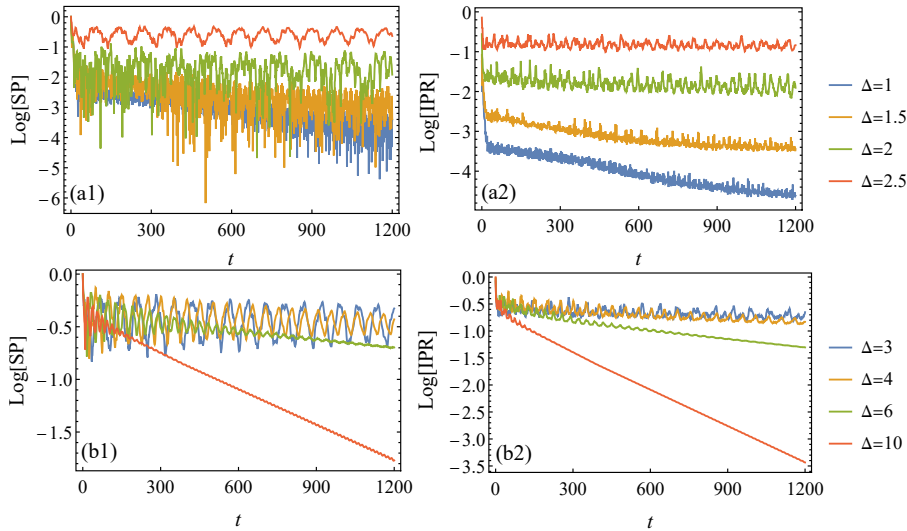


Figure 1: (Color online) Logarithmic plotting for the time evolution of SP (right column) and IPR (left column) when $a = 0$ for different values of Δ . The initial state is chosen as the highest excited state of H_S in all plots. For these plots, $\eta = 0.1$, $\omega_c = 10$, $s = 1$ and $\phi = \pi$ are chosen.

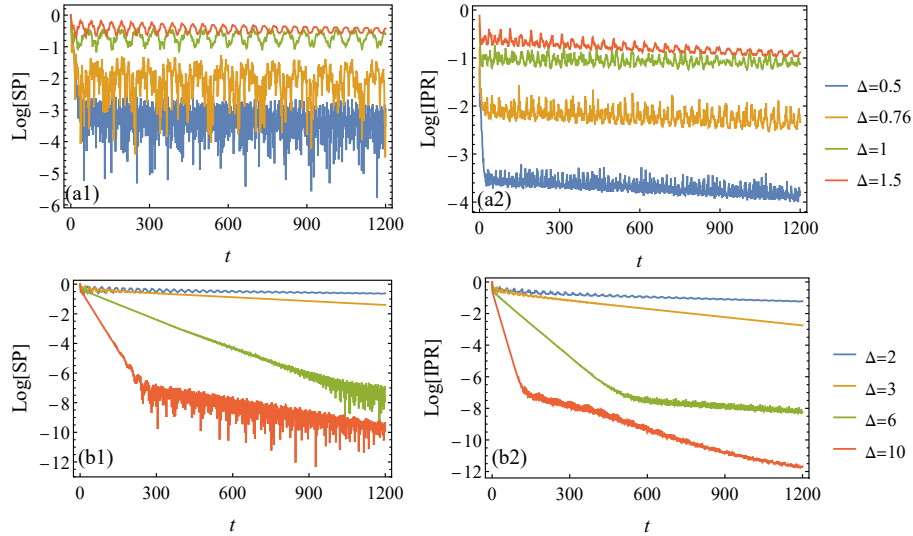


Figure 2: (Color online) Logarithmic plotting for the time evolution of SP (right column) and IPR (left column) when $a = 0.5$ for different values of Δ . The initial state is chosen as the highest excited state of H_S in all plots. The other parameters are the same as those shown in Fig. 1.

shown in Fig. 2 (b1) and (b2). This feature is consistent with the observation in the case of $a = 0$. The strong localization of a state can enhance the lost of information within the initial state.

Similar to the former case, one can find that both SP and IPR seem to become numerically stable when $\Delta = 1$, as shown in Fig. 2 (a1) and (a2). Meanwhile, a regular oscillation can also be noted for SP. The stability can also be demonstrated by $\langle \delta^2 n \rangle$. As shown in Fig.A2(e) in Appendix, a regular oscillation of $\langle \delta^2 n \rangle$ can be observed. In contrast, this picture is absent for the other value of Δ , as exemplifications in Fig. A2(d) and (f).

To conclude, we have shown that the localization does

not always preserve the excitation in the system. Instead, strong localization enhances the decaying of excitation into the environment. However, one can also note that before this picture occurs, a stability of SP or IPR can be found. This observation implies that the localization enhanced dissipation could have different underlying physical reason that will be disclosed in the next section.

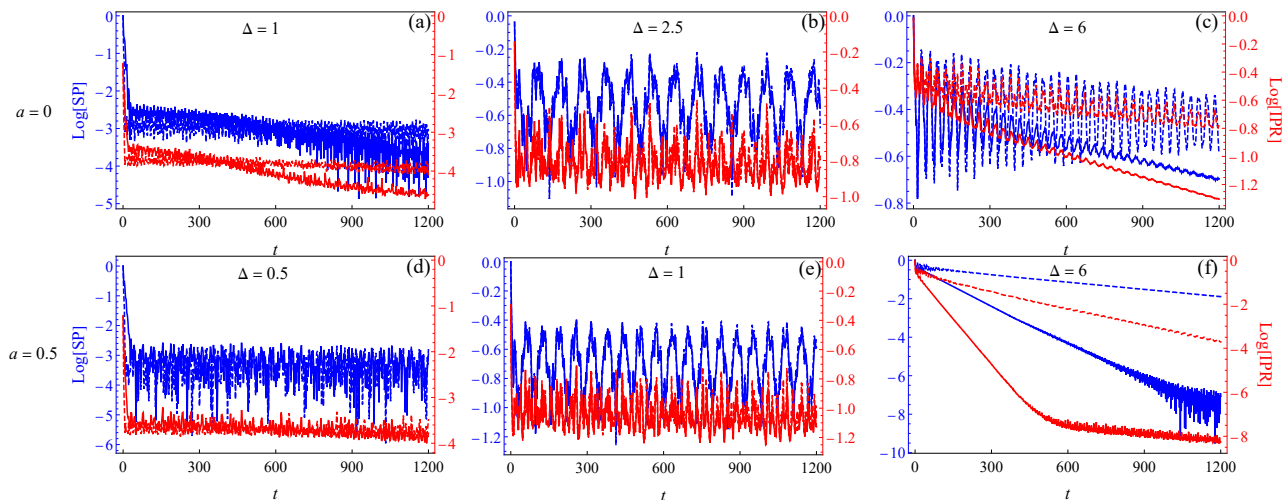


Figure 3: (Color online) Comparative plotting of the time evolution of SP (blue color) and IPR (red color) for $\eta = 0.1$ (solid line) and $\eta = 0.5$ (dashed line). Except for a and Δ , $\omega_c = 10$, $s = 1$ and $\phi = \pi$ are selected for all plots.

IV. COUPLING INDUCED COHERENT TRANSITION AMONG ENERGY LEVEL E_S

In general, the periodic oscillation of SP is a manifestation of the coherent transition between two orthogonal states. To verify this point, it is necessary to find the eigenstates by solving the Schrödinger equation as follows:

$$H|\psi_E\rangle = E|\psi_E\rangle, \quad (10)$$

in which $H = H_S + H_B + H_{int}$ is the total Hamiltonian of the system plus its environment. Formally, the eigenstate can be written as $|\psi_E\rangle = \left(\sum_{n=1}^N \alpha_n |1\rangle_n |0\rangle^{\otimes(N-1)}\right) \otimes |0\rangle^{\otimes M} + |0\rangle^{\otimes N} \otimes \left(\sum_{k=1}^M \beta_k |1\rangle_k |0\rangle^{\otimes(M-1)}\right)$. Substituting $|\psi_E\rangle$ into Eq. (10) and eliminating β_k , we get

$$(\alpha_{n+1} + \alpha_{n-1}) + \Delta \cos(2\pi\beta n + \phi)\alpha_n + \int_0^\infty d\omega \frac{J(\omega)}{E - \omega} \sum_{n=1}^N \alpha_n = E\alpha_n. \quad (11)$$

By solving Eq.(11), the eigenenergy E and the corresponding coefficient α_n can be determined, which characterizes the state of system after tracing out the environment. In this sense, we call the state $\sum_n \alpha_n |1\rangle_n$ as the reduced energy eigenstate of system. As shown in Appendix, because of the integral $\int_0^\infty d\omega \frac{J(\omega)}{E - \omega}$, E can be complex, and thus Eq.(11) depicts the nonunitary dynamics of single excitation in the atomic chain. Formally, one can introduce an effective non-Hermitian Hamiltonian to characterize the nonunitary dynamics. In this point, the state $\sum_n \alpha_n |1\rangle_n$ can be considered as the eigenstate of the non-Hermitian Hamiltonian. However, it is difficult to construct the counterpart in this case since E is involved in Eq. (11). Thus, in order to find E and corresponding α_n s, one has to resort to numerical method.

In Appendix, Eq. (11) is solved numerically for $a = 0$, $\Delta = 2.5$ and $a = 0.5$, $\Delta = 1$ respectively. Focusing on two highest E , we found that the difference of their real parts is consistent with the oscillation frequency of SR, observed in previous section. For instance, it is found for $a = 0$ and $\Delta = 2.5$ that the oscillation of SR has a frequency of $\sim 2\pi/77.8 = 0.08076$. Correspondingly, the calculated difference between the real parts of two highest E s is $2.952238 - 2.882305 = 0.069933$, as shown in Fig. 3(a). Similar observation can also be found for $a = 0.5$ and $\Delta = 1$, that SR shows an oscillation with frequency $\sim 2\pi/57.6 = 0.109083$. The calculated difference is $2.705113 - 2.605926 = 0.099187$, as shown in Fig. 3(b). The small discrepancy can be attributed to the error of estimation. Moreover, it is noted that the imaginary part of the highest E has a order of magnitude $\sim 10^{-6}$ in both cases. This means that the decaying of SP and IPR is slow and neither display a discernable descent in numerical simulation up to $t \sim 10^3$. In further, we also calculate the overlap between the initial state of system and the state $|\psi_{ES}\rangle$ corresponding to the highest E . For $a = 0$, $\Delta = 2.5$, $|\langle ES|\psi_{ES}\rangle|^2 = 0.498776$, which is consistent to the extremal maximum of SP 0.496809 extracted from the data in Fig. 1. While for $a = 0.5$, $\Delta = 1$, $|\langle ES|\psi_{ES}\rangle|^2 = 0.4471716$, which is consistent to the extremal maximum of SP 0.405453 extracted from the data in Fig. 2.

We have shown that the steady oscillation of SP comes from the coherent transition of system between two highest excited states. Physically, the transition is a consequence of the energy exchange between the system and its environment. Thus it is expected that the transition can be varied by changing the coupling strength η . A comparative study of SP or IPR is presented for $\eta = 0.1$ (the solid line) and $\eta = 0.5$ (the dashed line) in Fig. 3. It is clear that SP or IPR may show distinct response to the increasing of η , depending on the localization of

initial state. For initial state being extended or weakly localized, the evolution of both SP and IPR display small variation for different η , as shown in Fig.3 (a) and (d). In contrast, for initial state being highly localized, a significant variation of SP and IPR can be observed. As shown in Figs.3 (c) and (f), the evolution of SP or IPR can be stretched significantly by increase of η . Especially, an oscillation is developed with increase of η , as demonstrated in Fig.3 (c). However, for the steady cases displayed in the previous section, the increase of coupling strength has no noticeable effect on SP or IPR, as shown in Figs.3 (b) and e. In order to explain this phenomenon, we also examine the two highest E s for different Δ or η , as shown in Table I. It is noted that the difference between real parts of the two highest E s is enlarged with increase of Δ or η .

Combined with these observations together, one can conclude that the localization enhanced decaying of excitation is a consequence that the environment is unable to provide suitable energy to drive the coherent transition of excitation between the states corresponding to the two highest E , since their energy gap become large with increase of Δ . As a result, the energy would unidirectionally flow into the environment, and the excitation may be absorbed completely by environment. Whereas for ES being extended or weakly localized, the energy gap is small. Thus, the environment provides excessive energy such that make ES interfered with more than one energy level of system. As a result, the excitation might be populated in the entire atomic sites, and the information of initial state becomes erased rapidly. The increase of η enhances the energy exchange between the system and its environment. This is the reason that SP or IPR becomes stretched as shown in Figs.3 (c) and (f).

V. CONCLUSION

In conclusion, the exact dynamics of excitation, initially embedded in the highest excited state of a GAAH model coupled to an Ohmic-type environment, is studied by evaluating SP and IPR. An important observation is that the stable oscillation and the enhanced decaying of SP and IPR can be detected when the localization of the initial state is moderate or strong. This finding is distinct from the common perception that the localization in the system would protect quantum information against dissipation. To gain a further understanding of this result, the eigen energy E is determined analytically by solving Eq. (11). It is shown that the stable oscillation of SP and IPR is a result of the coherent transition of excitation between the states corresponding the two highest E s, which stems from the energy exchange between the system and the environment. Consequently, the environment can feed back appropriate energy into the system, which induces a periodic population of the system on the two states. However, with the substantial increase of Δ , the energy difference between these

$a = 0$		
η	0.1	0.5
$\Delta = 1$	$2.0671 - 1.4187 \times 10^{-10}i$	$2.0671 - 2.8230 \times 10^{-11}i$
	$2.0591 - 5.8097 \times 10^{-8}i$	$2.05910 - 1.1555 \times 10^{-8}i$
$\Delta = 2.5$	$2.9522 - 5.0623 \times 10^{-6}i$	$2.9522 - 1.0123 \times 10^{-6}i$
	$2.8823 - 5.3124 \times 10^{-5}i$	$2.8822 - 1.0584 \times 10^{-5}i$
$\Delta = 6$	$6.1522 - 3.3326 \times 10^{-4}i$	$6.1519 - 6.7207 \times 10^{-5}i$
	$5.9587 - 4.0397 \times 10^{-3}i$	$5.9539 - 8.2535 \times 10^{-4}i$
$a = 0.5$		
η	0.1	0.5
$\Delta = 0.5$	$2.1666 - 2.7500 \times 10^{-8}i$	$2.1666 - 5.4767 \times 10^{-9}i$
	$2.1365 - 5.3164 \times 10^{-8}i$	$2.1365 - 1.0566 \times 10^{-8}i$
$\Delta = 1$	$2.7051 - 7.0911 \times 10^{-6}i$	$2.7051 - 1.4174 \times 10^{-6}i$
	$2.6059 - 6.0298 \times 10^{-5}i$	$2.6058 - 1.1989 \times 10^{-5}i$
$\Delta = 6$	$11.9802 - 0.01578i$	$11.9766 - 3.2128 \times 10^{-3}i$
	$11.3612 - 0.1374i$	$11.3003 - 0.0305i$

Table I: A comparison of the two highest E when $\eta = 0.1$ and $\eta = 0.5$. The value of E is determined numerically by solving Eq. (11). The other parameters are same as those in Fig. 3

two states is enlarged. Thus, the environment could not feed back enough energy to give rise to population. In contrast, when the energy difference is small for, the feedback of energy from environment would make the highest level interfered with the other levels. As a consequence, the information of initial state is eventually erased. This explanation is further verified by establishing the influence of the coupling strength η . As shown in Fig. 3 (c) and (f), the increase of η significantly stretches decaying of both SP and IPR when the highest energy level E is strongly localized. Whereas for the highest energy level being extended or weakly localized, the increase of η generally enhances the decaying of SP and IPR at a short time, as shown in Fig. 3 (a) and (d).

Finally, it should be pointed out that the appearance of particle interaction can significantly modify the dynamics of excitation in the system. However, the exact treatment of open dynamics in the context of interacting many-body systems is a challenging task. Recent studies on disordered many-body systems showed that the role of interaction is to delocalize the system [1, 5]. In this sense, the interaction could act as an environment, which thermalizes the system. Concerning the fact that the localization-enhanced dissipation is state-dependent only, it may still be observed even if the interaction happens.

Acknowledgments

HTC acknowledges the support of Natural Science Foundation of Shandong Province under Grant No. ZR2021MA036. MQ acknowledges the support of Na-

tional Natural Science Foundation of China (NSFC) under Grant No. 11805092 and Natural Science Foundation of Shandong Province under Grant No. ZR2018PA012. HZS acknowledges the support of NSFC under Grant No.11705025. XXY acknowledges the support of NSFC under Grant No. 11775048.

Appendix

The integral $\int_0^\infty d\omega \frac{J(\omega)}{E-\omega}$ in Eq. (11) is divergent when $E > 0$. Therefore, to determine E , we apply the Sokhotski-Plemelj (SP) formula to evaluate the above integral. The SP formula can be given as

$$\lim_{\epsilon \rightarrow 0} \frac{1}{x - x_0 \pm \pm i\epsilon} = P \frac{1}{x - x_0} \mp i\pi\delta(x - x_0), \quad (\text{A1})$$

in which P denotes the principle value of Cauchy. Thus,

$$\lim_{\epsilon \rightarrow 0} \int_0^\infty d\omega \frac{J(\omega)}{\omega - E - i\epsilon} = P \int_0^\infty d\omega \frac{J(\omega)}{\omega - E} + i\frac{\pi}{2} J(E) \quad (\text{A2})$$

In the above derivation, the case of $-i\epsilon$ is selected. As shown in the following discussion, this choice guarantee E has a negative imaginary part that characterizes dynamic dissipation.

The value of E can be established by finding zero coefficient determinants in Eq. (11). In Fig. A1, the contour plots for the vanishing real (solid- blue line) and imaginary (dashed- red line) part of coefficient determinant

are presented, respectively, for (a) $a = 0, \Delta = 2.5$ and (b) $a = 0.5, \Delta = 1$, in which the crossing point of the two lines corresponds to the value of reduced energy E . The two inner panels in each plot show the details for the two E s with the largest real part. The rigorous value of E and the corresponding α_n can be decided by recurrently solving the eigenvalue equation Eq. (10). By doing so, the result shows that $E_1 = 2.952238 - 5.062298 \times 10^{-6}i$, $E_2 = 2.882305 - 5.312399 \times 10^{-5}i$ for case (a) and $E_1 = 2.705113 - 7.091364 \times 10^{-6}i$, $E_2 = 2.605926 - 6.029 \times 10^{-5}i$ for case (b).

To characterize the stability of SP or IPR observed in Fig. 1 and 2, the variance of the position of excitation within the atomic site, defined as $\langle \delta^2 n \rangle = \frac{\sum_{n=1}^N |\alpha_n(t)|^2 (n - \langle n \rangle)^2}{\sum_n |\alpha_n(t)|^2}$ and $\langle n \rangle = \sum_n |\alpha_n(t)|^2 n$, is studied for different cases in Fig. A2. It is evident that $\langle \delta^2 n \rangle$ can display regular oscillation for $a = 0, \Delta = 2.5$ and $a = 0.5, \Delta = 1$. This feature can also be understood from the coupling induced coherent transition of the two highest energy levels, as a result of which $\langle \delta^2 n \rangle$ would be determined by the two levels. In contrast, for $a = 0, \Delta = 1$ and $a = 0.5, \Delta = 0.5$, the time evolution of $\langle \delta^2 n \rangle$ becomes irregular. This observation can be attributed to the extensivity of the system, by which the excitation would populate uniformly in the atomic sites. However, for $a = 0, \Delta = 1$ and $a = 0.5, \Delta = 3$, the system is deeply in the localized phase. Thus, one can find that $\langle \delta^2 n \rangle$ tends to be stable as shown in Fig. A2.

-
- [1] P. W. Anderson, *Absence of diffusion in certain random lattices*, Phys. Rev. **109**, 1492-1505(1958); R. Nandkishore, and D. A. Huse, *Many-body localization and thermalization in quantum statistical mechanics*. Annu. Rev. Condens. Matter Phys. **6**, 15 (2015); D. A. Abanin, E. Altman, I. Bloch, and M. Serbyn, *Colloquium: many-body localization, thermalization, and entanglement*, Rev. Mod. Phys. **91**, 021001 (2019).
- [2] M. Schulz, C. A. Hooley, R. Moessner, and F. Pollmann, *Stark many-body localization*, Phys. Rev. Lett. **122**, 040606 (2019); E. van Nieuwenburga, Y. Bauma, and G. Refaela, *From Bloch oscillations to many-body localization in clean interacting systems*, PNAS **116**, 9269-9274 (2019).
- [3] C. J. Turner, A. A. Michailidis, D. A. Abanin, M. Serbyn, and Z. Papić, *Weak ergodicity breaking from quantum many-body scars*, Nat. Phys. **14**, 745-749 (2018); *Quantum scarred eigenstates in a Rydberg atom chain: Entanglement, breakdown of thermalization, and stability to perturbation*, Phys. Rev. B **98**, 155134 (2018).
- [4] P. Sala, T. Rakovszky, R. Verresen, M. Knap, and F. Pollmann, *Ergodicity Breaking Arising from Hilbert Space Fragmentation in Dipole-Conserving Hamiltonians*, Phys. Rev. X **10**, 011047 (2020); F. Pietracaprina, N. Laflorencie, *Hilbert Space Fragmentation and Many-Body Localization*, Phys. Rev. Lett. **124**, 207602 (2020).
- [5] M. Schreiber, S. S. Hodgman, P. Bordia, H. P. Lüschen, M. H. Fishcher, R. Vosk, E. Altman, U. Schneider, and I. Bloch, *Observation of Many-body Localization of interacting Fermions in a Quasirandom Optical Lattice*, Science **349**, 842-845 (2015).
- [6] P. Roushan, C. Neill, J. Tangpanitanon, *et.al.*, *Spectroscopic signatures of localization with interacting photons in superconducting qubits*, Science **358**, 1175-1179 (2017); M. Gong, G. D. de Morases Neto, C. Zha, *et.al.*, *Experimental characterization of quantum many-body localization transition*, arXiv:2012.11521 [quant-ph] (2020).
- [7] E. Levi, M. Heyl, I. Lesanovsky, and J. P. Garrahan, *Robustness of many-body localization in the presence of dissipation*, Phys. Rev. Lett. **116**, 237203 (2016); M. H. Fischer, M. Maksymenko, and E. Altman, *Dynamics of a many-body-localized systems coupled to a bath*, Phys. Rev. Lett. **116**, 160401 (2016); I. Yusipov, T. Lapyteva, S. Denisov, and M. Ivanchenko, *Localization in Open Quantum Systems*, Phys. Rev. Lett. **118**, 070402 (2017); L.-N. Wu and A. Eckardt, *Bath-induced decay of Stark many-body-localization*, Phys. Rev. Lett. **123**, 030602 (2019).
- [8] H. P. Lüschen, P. Bordia, S. S. Hodgman, M. Schreiber, S. Sarkar, A. J. Daley, M. H. Fischer, E. Altman, I. Bloch, and U. Schneider, *Signature of many-body localization in a controlled open quantum system*, Phys. Rev. X **7**, 011034 (2017).

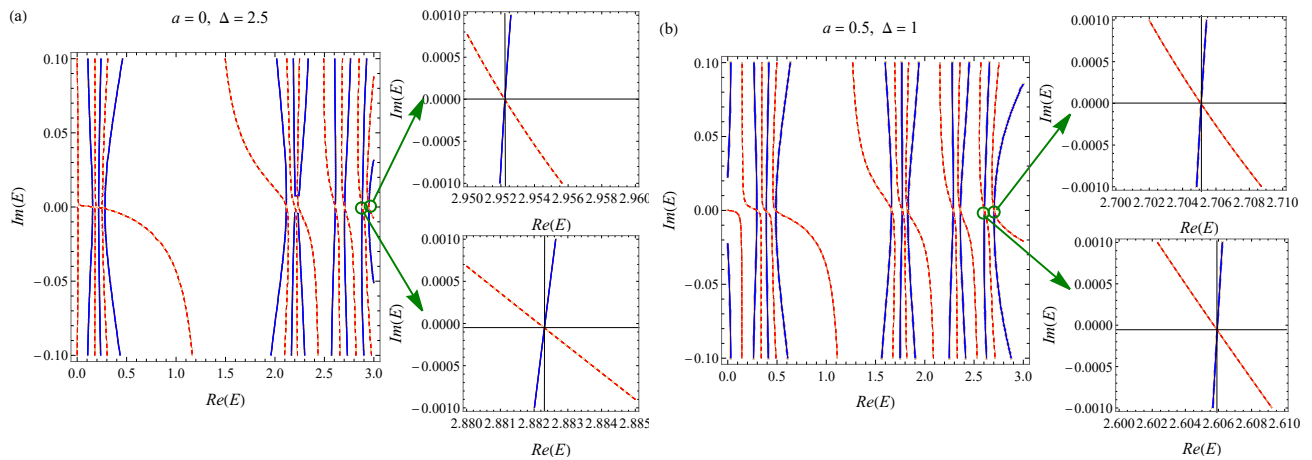


Figure A1: (Color online) The contour plots of numerical determination of E in Eq. (11) when (a) $a = 0, \Delta = 2.5$ and (b) $a = 0.5, \Delta = 1$. The solid-blue and dashed-red line panels represent respectively the vanishing real and imaginary part of the coefficient determinant in Eq. (11). The inner panels in (a) and (b) decide the two highest reduced energy levels. $\eta = 0.1$, $\omega_c = 10$, $s = 1$ and $\phi = \pi$ are chosen for these plots

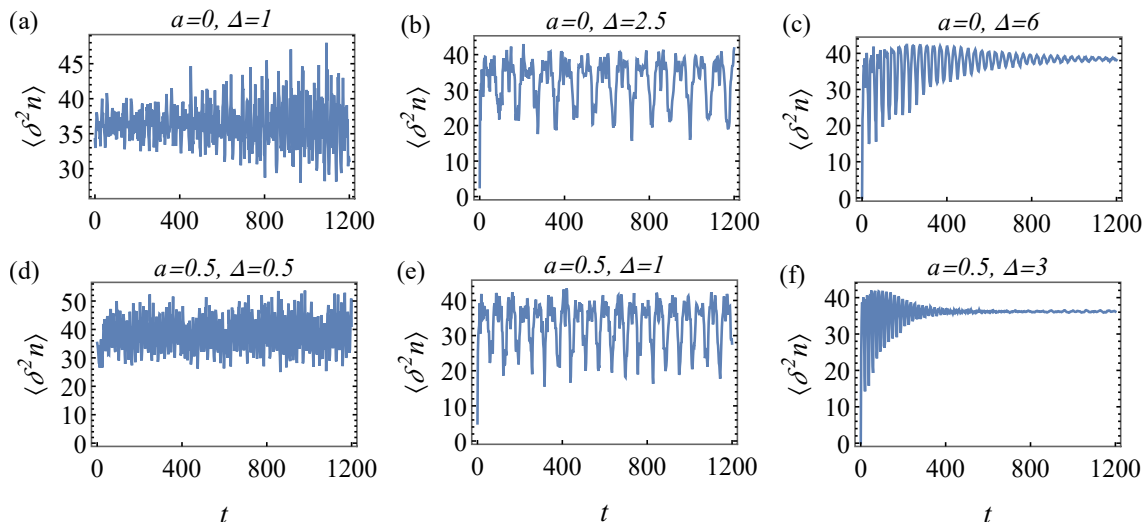


Figure A2: (Color online) The plots of $\langle \delta^2 n \rangle$ for different situations. Except of a and Δ , $\eta = 0.1$, $\omega_c = 10$, $s = 1$ and $\phi = \pi$ are chosen for these plots.

- [9] L. Levi, M. Rechtaman, B. Freedman, T. Schwartz, O. Manela, and M. Segev, *Disorder-enhanced transport in photonic quasicrystals*, Science **332**, 541-544 (2011); S. Longhi, *Inverse Anderson transition in photonic cages*, Opt. Lett. **46**, 2872-2875 (2021).
- [10] E. Zerah-Harush and Y. Dubi, *Effect of disorder and interactions in environment assisted quantum transport*, Phys. Rev. Research, **2**, 023294 (2020); N. C. Cháves, F. Mattiotti, J. A. Méndez-Bermúdez, F. Borgonovi, and G. Luca Celardo, *Disorder-enhanced, and disorder-independent transport with long-range hopping: application to molecular chains in optical cavities*, Phys. Rev. Lett. **126**, 153201 (2021); D. Dwiputra, and F. P. Zen, *Environment-assisted quantum transport and mobility edges*, arXiv: 2012.09337 [quant-ph] (2020).
- [11] S. Ganeshan, J. H. Pixley, and S. Das Sarma, *Nearest neighbor tight binding models with an exact mobility edge in one dimension*, Phys. Rev. Lett. **114**, 146601 (2015).
- [12] S. Aubry and G. André, *Analyticity Breaking and Anderson Localization in Incommensurate Lattices*, Ann. Isr. Phys. Soc. **3**, 33 (1980); P. G. Haper, *Single Band Motion of Conduction Electrons in a Uniform Magnetic Field*, Proc. Phys. Soc. London Sect. A **68**, 874 (1955).
- [13] F. Alex An, K. padavić, E. J. Meier, S. Hegde, S. Ganeshan, H. H. Pixley, S. Vishvershare, and B. Gadway, *Interaction and mobility edge: observing the generalized Aubry-Andeé model*, Phys. Rev. Lett. **136**, 040603 (2021).
- [14] A. J. Leggett, S. Chakravarty, A. T. Dorsey, Matthew P. A. Fisher, A. Garg, and W. Zwerger, *Dynamics of the dissipative two-state system*, Rev. Mod. Phys. **59**, 1-85 (1987).
- [15] H.-N. Xiong, W.-M. Zhang, X. Wang, and M.-H. Wu, *Exact non-Markovian cavity dynamics strongly coupled*

- to a reservoir, Phys. Rev. A **82**, 012105 (2010).
- [16] E. J. Torres-Herrera and Lea F. Santos, *Dynamics at the many-body localization transition*, Phys. Rev. B **92**, 014208 (2015).
- [17] E. Yablonovitch, *Inhibited Spontaneous Emission in Solid-State Physics and Electrics*, Phys. Rev. Lett. **58**, 2059-2062 (1987); S. John and J. Wang, *Quantum Electrodynamics near a Photonic Band Gap: Photon Bound States and Dressed Atoms*, Phys. Rev. Lett. **64**, 2418 - 2421 (1990).